PNAS RESEARCH ARTICLE | MEDICAL SCIENCES

Agonist of growth hormone-releasing hormone improves the disease features of spinal muscular atrophy mice

Marina Boido[a,1], Iacopo Gesmundo[b,1], Anna Caretto[a,1], Francesca Pedrolli[b], Roberta Schellino[a], Sheila Leone[c], Renzhi Cai[d,e], Wei Sha[d], Ezio Ghigo[b], Andrew V. Schally[d,e,f,g,h,2], Alessandro Vercelli[a,1], and Riccarda Granata[b,1,2]

Contributed by Andrew V. Schally; received October 1, 2022; accepted November 24, 2022; reviewed by Gianluigi Condorelli and Ana Garcera Teruel

Spinal muscular atrophy (SMA) is a severe autosomal recessive neuromuscular disease affecting children and young adults, caused by mutations of the survival motor neuron 1 gene (*SMN1*). SMA is characterized by the degeneration of spinal alpha motor neurons (αMNs), associated with muscle paralysis and atrophy, as well as other peripheral alterations. Both growth hormone-releasing hormone (GHRH) and its potent agonistic analog, MR-409, exert protective effects on muscle atrophy, cardiomyopathies, ischemic stroke, and inflammation. In this study, we aimed to assess the protective role of MR-409 in SMNΔ7 mice, a widely used model of SMA. Daily subcutaneous treatment with MR-409 (1 or 2 mg/kg), from postnatal day 2 (P2) to euthanization (P12), increased body weight and improved motor behavior in SMA mice, particularly at the highest dose tested. In addition, MR-409 reduced atrophy and ameliorated trophism in quadriceps and gastrocnemius muscles, as determined by an increase in fiber size, as well as upregulation of myogenic genes and inhibition of proteolytic pathways. MR-409 also promoted the maturation of neuromuscular junctions, by reducing multi-innervated endplates and increasing those mono-innervated. Finally, treatment with MR-409 delayed αMN death and blunted neuroinflammation in the spinal cord of SMA mice. In conclusion, the present study demonstrates that MR-409 has protective effects in SMNΔ7 mice, suggesting that GHRH agonists are promising agents for the treatment of SMA, possibly in combination with SMN-dependent strategies.

GHRH agonists | alpha motor neurons | neuroinflammation | neuromuscular junction | spinal muscular atrophy

Significance

Spinal muscular atrophy (SMA) is a motor neuron (MN) degenerative disease and the main genetic cause of infant mortality, resulting from deficiency of survival motor neuron (SMN) protein. Growth hormone-releasing hormone (GHRH) and its agonistic analog MR-409 counteract muscle atrophy and exert potent cardioprotective, neuroprotective, and anti-inflammatory functions. Here, we report that treatment with MR-409 induced weight gain, improved motor behavior, attenuated muscle fiber atrophy and promoted the maturation of neuromuscular junctions in a mouse model of SMA. Furthermore, MR-409 prevented the loss of αMNs and decreased neuroinflammation in the spinal cord. Our findings demonstrate that MR-409 reduces the severity of SMA and may represent a potential new therapy for this disease.

Spinal muscular atrophy (SMA) is an autosomal recessive neuromuscular disorder and the leading genetic cause of infant death, with an incidence of around 1 in 6,000 to 10,000 live births (1, 2). SMA results from deletion or mutation of survival motor neuron 1 gene (*SMN1*) (3). In SMA patients, the loss of *SMN1* is only partially compensated by the centromeric paralogue *SMN2*, which encodes for only a 10% of the functional SMN protein and mainly produces a truncated form lacking exon 7 (SMNΔ7), that is rapidly degraded (4). The severity of SMA is inversely correlated with *SMN2* copy number and SMN protein levels, ranging from the most severe SMA I to the mildest SMA IV, according to the age of symptom onset and the disease progression (2, 3, 5).

The loss of SMN mainly affects alpha motor neurons (αMNs) in the brainstem and ventral horns of the spinal cord, resulting in progressive skeletal muscle weakness and atrophy and leading, in the most severe cases, to premature death (2, 6). Although classified as a MN disease, studies indicate that the lack of SMN can affect other cells and districts (7). In fact, non-neuronal cells, such as glial cells, muscles, and sensory afferent connections, have been implicated in SMA pathogenesis (5, 8–10). Moreover, emerging evidence suggests SMA as a multisystemic disease, encompassing defects in peripheral organs, including the heart, vasculature, lung, pancreas, liver, intestines, and bone (5, 7).

Therapeutic approaches for all SMA types have mainly focused on increasing available SMN protein. Current therapies include small molecules and antisense oligonucleotides (ASOs) that modify *SMN2* splicing, thereby promoting inclusion of exon 7 in SMN2 messenger RNA (mRNA), as well as gene therapy with adeno-associated virus 9 vectors (scAAV9) that deliver the *SMN1* complementary DNA (cDNA) to infected cells (11–13). However, although effective, these approaches have some limitations, such as unknown long-term effects, high costs, poor efficacy in milder or late-treated patients, disregarding SMN-independent targets and adverse effects (14). Thus, new therapeutic strategies are needed and combined therapies with other drugs should also be envisaged (12, 13, 15).

The hypothalamic peptide hormone growth hormone-releasing hormone (GHRH) stimulates the synthesis and release of GH from the anterior pituitary (16). GHRH also exerts many extrapituitary functions through GHRH receptors (GHRH-Rs), expressed in different cells and tissues. The peripheral activities of GHRH include anti-inflammatory,

Reviewers: G.C., Humanitas University; and A.G.T., Universitat de Lleida-IRBLleida.

Competing interest statement: The authors have patent filings to disclose, A.V.S., W.S. and R.C. are co-inventors on the patents for GHRH agonists, assigned to the University of Miami and Veterans Affairs Medical Center.

[1]M.B., I.G., A.C., A.V., and R.G. contributed equally to this work.

[2]To whom correspondence may be addressed. Email: Andrew.Schally@va.gov or riccarda.granata@unito.it.

This article contains supporting information online at https://www.pnas.org/lookup/suppl/doi:10.1073/pnas.2216814120/-/DCSupplemental.

Published January 5, 2023.

neuroprotective, and cardioprotective effects (17–20). In addition, our group previously demonstrated that GHRH counteracts tumor necrosis factor-α (TNF-α)-induced skeletal muscle atrophy, by promoting myotube survival and preventing proteolytic degradation (21). Many synthetic GHRH agonistic analogs of JI and MR class, have been synthesized in the last few decades in the laboratory of one of us (A.V.S.), with long half-life and high stability and activity and with no effect on GH axis-induced tumor growth (17, 22). Moreover, different studies have demonstrated that among MR analogs, MR-409 promotes cardioprotection (23–25), improves metabolic functions in diabetic mice (26), and displays neuroprotective effects in experimental models of diabetic retinopathy, ischemic stroke, and inflammation, also inducing anxiolytic and antidepressant-like behavior (27–29).

In the light of these premises, we investigated the effects of treatment with MR-409 in SMNΔ7 mice, an experimental model of SMA II (30, 31). We focused on the protective effects of MR-409 in skeletal muscle and spinal cord, by evaluating motor performance, muscular trophism, neuromuscular junction (NMJ) maturation/innervation, as well as MN survival and astrogliosis. The molecular pathways involved in the effects of MR-409 and the capacity to extend the lifespan were also investigated.

Results

MR-409 Increases Body Weight and Reduces the Severity of Motor Deficits in SMA Mice. The effects of MR-409 in SMA were studied in SMNΔ7 mice, *SMNΔ7*$^{+/+}$; *SMN2*$^{+/+}$; *Smn*$^{-/-}$ (designated SMA mice from now on). SMA mice were randomly assigned to receive a daily subcutaneous (s.c.) injection of either vehicle (VHL), 1 mg/kg MR-409 (MR-1) or 2 mg/kg MR-409 (MR-2), from P2 to sacrifice (P12). Until P7, the body weight gain of VHL mice was moderate and gradually increased between P8 and P10, when it reached the maximum value, decreasing thereafter. Conversely, treatment with MR-409 showed a dose-dependent weight increase, particularly evident with MR-2 for the entire period of observation, reaching the highest value at P10 (VHL: 3.50 ± 0.25 g; MR-2: 4.78 ± 0.22 g) (Fig. 1 *A* and *B*). To investigate whether MR-409 improves motor performance, SMA pups underwent a battery of behavioral tests from day P2 to P12. In the tail suspension test, MR-2 group showed a significant improvement in hindlimb posture at P6, with a score of 3.3 ± 0.26 compared with age-matched VHL mice (2.17 ± 0.30). The highest value was reached at P8 (3.56 ± 0.13) vs. VHL (2.57 ± 0.20), while declining at P10 and P12. MR-1 mice sustained the performance until P8, but did not reach the statistical significance (Fig. 1*C*). In the hindlimb suspension test, measured as latency to fall, treatment with MR-1 was the most effective, showing a significant improvement of the performance at P4, P6, and P10, while declining thereafter (Fig. 1*D*). In the righting reflex, MR-1 induced a slight but not significant improvement at P8 vs. VHL (17.17 ± 3.95 s vs. 28.36 ± 1.64 s). In the MR-2 group, while the performance was only slightly better than controls in the first days, from P10 it gradually improved, overlapping the latency time of MR-1 mice at P10 and P12, although being not statistically significant (Fig. 1*E*). Moreover, by evaluating the percentage of mice able to complete the test, MR-1 pups had, in general, less difficulties in righting themselves compared with VHL, in particular at P6, when the statistical significance is reached (Fig. 1*E′*). Finally, in the negative geotaxis test, while VHL mice never completed the test, the ability of both MR-1 and MR-2 pups in reorienting themselves gradually increased during the days. Nevertheless, at P12 the performance of MR-1 group slightly worsened (38.67 ± 6.56 s), whereas that of MR-2 further improved (28.87 ± 6.10 s) (Fig. 2*F*). The same trend was highlighted by calculating the percentage of mice that successfully completed the test (Fig. 2*F′*). Overall, these results indicate that 2 mg/kg MR-409 (MR-2) is the most effective dose, not only in promoting body weight gain, but also in improving tail suspension and negative geotaxis, in terms of posture, coordination, strength, and vestibular reflexes.

MR-409 Reduces Muscle Atrophy in SMA Mice. Muscle atrophy in SMA is primarily caused by reduced functional innervation; however, muscle-autonomous alterations also occur and could contribute to the pathogenesis of the disease (5, 11, 32, 33). Based on the beneficial effects of MR-409 on body weight gain and motor performance, we next evaluated whether MR-409 counteracts muscle atrophy in SMA mice. We first demonstrated the presence of GHRH-R protein in quadriceps and gastrocnemius, as well as in spinal cord of SMA mice (*SI Appendix*, Fig. S1 *A* and *B*). The morphology of quadriceps and gastrocnemius was next analyzed at P12 by hematoxylin and eosin staining on transverse sections (Fig. 2*A*), while morphometric analysis was performed using Neurolucida software. Mice treated with MR-409 showed a significant dose-dependent increase in fiber size of both quadriceps and gastrocnemius, assessed as mean fiber area (Fig. 2 *B* and *E*), perimeter (Fig. 2 *C* and *F*) and maximum Feret's diameter (Fig. 2 *D* and *G*), compared with VHL-treated animals, as well as with wild type (WT) animals. Interestingly, treatment with MR-2 resulted in an almost complete rescue of SMA muscle phenotype (*SI Appendix*, Tables S1 and S2). These results indicate that MR-409, particularly at 2 mg/kg, prevents muscle atrophy in SMA mice.

MR-409 Restores the Myogenic Program and Prevents Muscle Protein Degradation in SMA Mice. Muscle weakness in SMA has been associated with dysregulation of the myogenic program and profound deficits in muscle fiber growth and maturation or muscle maintenance (11, 32, 34, 35). Therefore, we assessed the role of MR-409 on gene expression of myogenic regulatory factors, such as myoblast determination 1 (*Myod1*) and myogenin (*Myog*), early and late markers of muscle differentiation, respectively (36), in quadriceps and gastrocnemius of P12 SMA mice. Treatment with MR-409 promoted an increase in Myod1 and Myog mRNA levels in both quadriceps (Fig. 3*A*) and gastrocnemius (Fig. 3*B*), particularly at 2 mg/kg, compared with VHL. MR-409 also upregulated myosin heavy chain (*Myh*) isoforms, which are involved in muscle contraction and are altered in SMA (37). In fact, MR-2 produced a strong increase in postnatal *Myh1* (encoding for fast MyHC-2x), postnatal *Myh2* (fast MyHC-2a), embryonic *Myh7* (slow MyHC-I) and embryonic *Myh8* (MyHC-pn) in both muscles, whereas MR-1 showed little or no effect (Fig. 3 *A* and *B*). In both quadriceps (Fig. 3 *C* and *E*) and gastrocnemius (Fig. 3 *D* and *F*), MR-409 also reduced the mRNA and protein levels of atrogin-1 and the proteolytic E3 ubiquitin ligases muscle ring finger 1 (MuRF1) and, also known as atrogenes (i.e., related to muscle atrophy), which are upregulated in SMA (38). Together, these data suggest that MR-409 attenuates the disruption of the myogenic program and counteracts muscle atrophy in SMA mice.

MR-409 Promotes the Maturation of NMJs in SMA Mice. Along with muscular atrophy, dramatic alterations in maturation and function of NMJs have been observed in both SMA mice and humans, including the presence of immature (multi-innervated) and denervated NMJs (5, 39). To verify the effect of MR-409 on NMJ innervation, longitudinal sections of

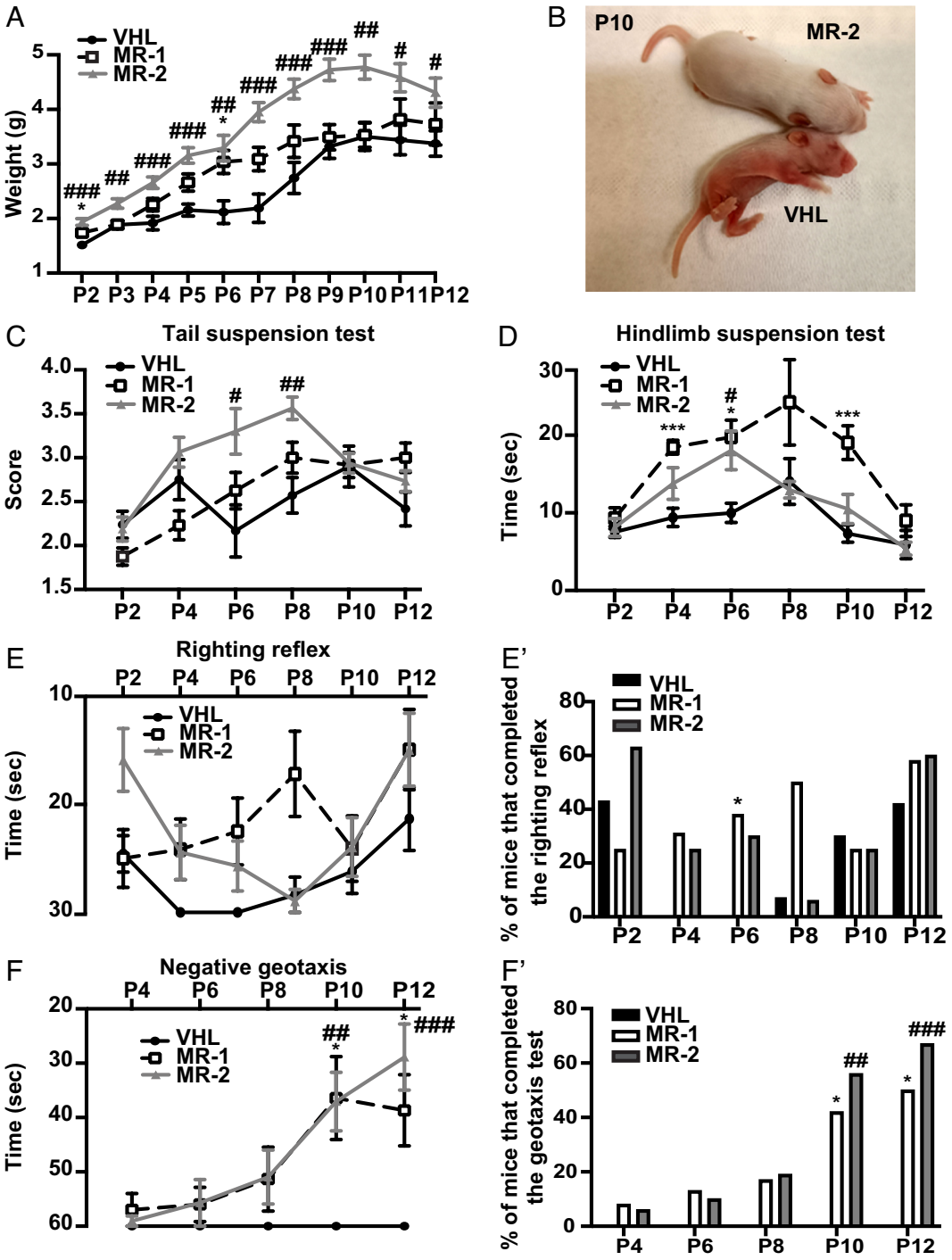

Fig. 1. Effect of MR-409 on body weight and motor performance in SMA mice. (*A*) Body weight evaluated at the indicated postnatal days (P) in mice treated with either vehicle (VHL: $n = 21$), 1 mg/kg MR-409 (MR-1: $n = 13$) or 2 mg/kg MR-409 (MR-2: $n = 16$). Data are mean ± SEM. $^{*}P < 0.05$ for MR-1 vs. VHL; $^{\#}P < 0.05$; $^{\#\#}P < 0.01$, $^{\#\#\#}P < 0.001$ for MR-2 vs. VHL by repeated-measures ANOVA, mixed-effects model with Geisser-Greenhouse correction and Tukey's post hoc test. (*B*) Representative image showing differences in body size between VHL and MR-2 mice at P10. Motor performance in treated or untreated SMA mice assessed by tail suspension test (*C*), hindlimb suspension test (*D*) righting reflex (*E* and *E'*) and negative geotaxis (*F* and *F'*) (VHL: $n = 21$; MR-1: $n = 13$; MR-2: $n = 16$). Data are mean ± SEM. $^{*}P < 0.05$, $^{***}P < 0.001$ for MR-1 vs. VHL; $^{\#}P < 0.05$; $^{\#\#}P < 0.01$, $^{\#\#\#}P < 0.001$ for MR-2 vs. VHL by repeated-measures ANOVA, mixed-effects model with Geisser-Greenhouse correction and Tukey's post hoc test (for *C*–*F*), and Fisher's exact test (for *E'* and *F'*).

quadriceps and gastrocnemius from P12 SMA mice were stained with α-bungarotoxin (α-BTX) and anti-neurofilament (NF) antibody. We assessed the number of NFs reaching the endplates, by classifying NMJs as multi-innervated (two or more NFs), mono-innervated (only one NF) or denervated (no NFs) (Fig. 4*A*). Treatment with the highest dose of MR-409 blunted the percentage of multi-innervated endplates in both muscles, although was statistically significant only in quadriceps, compared with VHL (Fig. 4 *B*, *C*, and *F*). Furthermore, MR-409 induced a dose-dependent increase in mono-innervated (mature) endplates, with a significant effect observed with MR-2 (Fig. 4 *B*, *D*, and *G*). Concomitantly, the amount of denervated endplates was reduced by MR-2 and slightly, but not significantly, blunted also by MR-1 (Fig. 4 *B*, *E*, and *H*) (*SI Appendix*, Tables S3 and S4). Overall,

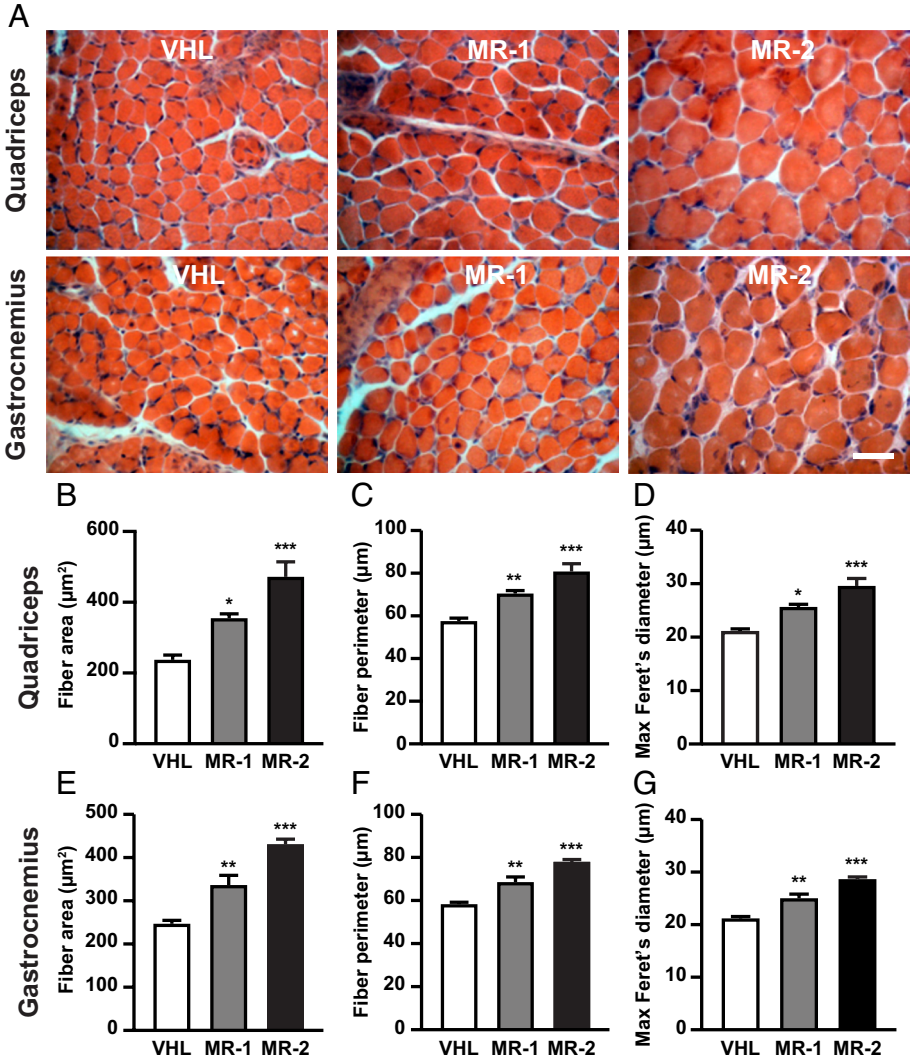

Fig. 2. Analysis of muscular fiber size in SMA mice treated with MR-409 at P12. (*A*) Representative hematoxylin/eosin staining of quadriceps and gastrocnemius transverse sections from mice, either untreated (VHL), treated with 1 mg/kg MR-409 (MR-1) or 2 mg/kg MR-409 (MR-2). (Scale bar, 30 µm.) Morphometric analysis of fiber area (*B* and *E*), perimeter (*C* and *F*) and maximum Feret's diameter (*D* and *G*) in quadriceps and gastrocnemius. (n = 5 for each group). Data are mean ± SEM. *P < 0.05, **P < 0.01, ***P < 0.001 vs. VHL by one-way ANOVA and Tukey's post hoc test.

these findings suggest that MR-409 promotes the maturation and delays the denervation process in NMJs of SMA mice.

MR-409 Attenuates the Loss of αMNs and Reduces Astrogliosis in Spinal Cord of SMA Mice. The improvement in skeletal muscle trophism and NMJ maturation prompted us to investigate whether MR-409 would protect against αMN degeneration and death, a key pathological feature of SMA (40, 41). Stereological counts of Nissl-stained αMNs were performed in lumbar spinal cord of P12 mice, comparing the treatment with MR-2, selected as the most protective dose, with VHL. The density of αMNs was preserved in MR-2 group more than in VHL (Fig. 5 *A*–*C*). Furthermore, we observed a small, nonsignificant increase of SMN protein in spinal cords of MR-2 mice compared with VHL (*SI Appendix*, Fig. S2). MR-2-induced protection was further assessed on astrogliosis, a neuroinflammatory process implicated also in SMA (9, 42). Immunostaining for glial fibrillary acidic protein (GFAP), a marker for astrocyte activation, was reduced in ventral horns of spinal cord of MR-2 group, compared with VHL (Fig. 5 *D*–*F*). Furthermore, real-time PCR analysis, performed on lumbar spinal cord samples, showed attenuation of inflammatory cytokines *TNF-α*, interleukin-1 beta (*IL-1β*), and interleukin-6 (*IL-6*) in MR-2 vs. VHL mice (Fig. 5*G*). These results suggest a protective role for MR-409 against αMN loss and neuroinflammation in SMA.

Effect of MR-409 on Survival of SMA Mice. Finally, in a different set of experiments, we aimed to determine the role of MR-409 on mice lifespan. Kaplan–Meier analysis demonstrated that treatment with MR-2 promoted a slight, but not significant, extension in median survival, compared with mice treated with VHL (MR-409: 16 d; VHL: 14 d) (Fig. 6).

Discussion

The present study demonstrates that treatment with GHRH agonistic analog MR-409 positively modifies the SMA phenotype in SMNΔ7 mice. Thus, MR-409 promoted body weight gain, improved motor performance, reduced muscle atrophy, increased NMJ maturation and attenuated the loss of MNs and astrogliosis.

It has been shown that both male and female SMA mice are significantly smaller than their normal littermates, due to muscle atrophy (30, 31). Our results show a strong increase in body

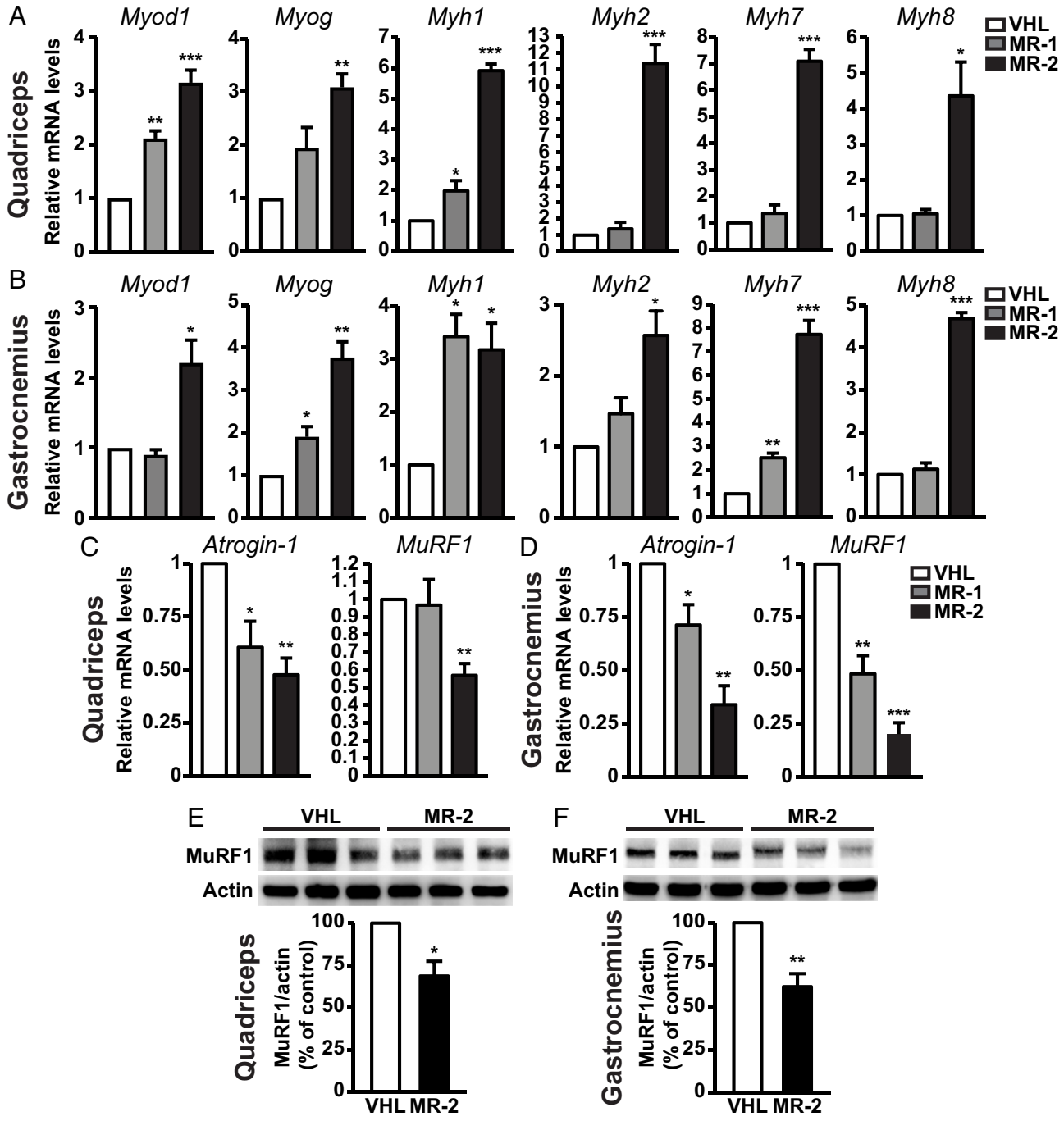

Fig. 3. Effect of MR-409 on expression of myogenic genes and atrophic factors in muscles of P12 SMA mice. Real-time PCR analysis for myogenic genes (*Myod1Myog*), myosin heavy chain isoforms (*Myh1, Myh2, Myh7* and *Myh8*) and atrogenes (*atrogin-1* and *MuRF1*) normalized to 18S rRNA in quadriceps (*A* and *C*) and gastrocnemius (*B* and *D*) of mice treated with either VHL, 1 mg/Kg MR-409 (MR-1) or 2 mg/kg MR-409 (MR-2). Data are mean ± SEM. $^{*}P < 0.05$, $^{**}P < 0.01$, $^{***}P < 0.001$ vs. VHL by one-way ANOVA and Tukey's post hoc test ($n = 5$ for each group). Representative western blots for MuRF1 in quadriceps (*E*) and gastrocnemius (*F*) of mice treated with VHL or MR-2. Actin served as internal control. Results, expressed as percentage of control (VHL), are mean ± SEM ($n = 3$ for each group).

weight in SMA mice treated with MR-409, particularly at the highest dose tested, an effect likely associated with the improvement in muscle trophism and neuromuscular function. In fact, while GHRH antagonists, such as MIA-690, can increase food intake in mice through activation of agouti-related peptide (AgRP) neurons (43), MR-409 does not exert similar effects. In addition, whereas peripherally-administered GHRH was inactive, intracerebroventricular (i.c.v.) injection either stimulated or inhibited feeding behavior (44, 45). Here, MR-409 was given subcutaneously in SMA mice, suggesting feeding-independent effect on weight increase; however, further studies are required to define better the role of MR-409 on hypothalamic feeding circuits. One of the major symptoms of SMA is the loss of muscle strength, which severely impairs motor behavior (2, 4–6); moreover, skeletal muscle has been reported to be profoundly damaged in SMA (32, 33). Furthermore, SMNΔ7 mice show a strong resemblance to SMA in humans in that they show a progressive loss of motor function (30). Our results on behavioral tests demonstrate that MR-409 improved overall muscle strength and coordination, as well as posture and vestibular reflexes, significantly delaying the disease onset and progression. These findings were paralleled with the partial recovery of myofiber size in quadriceps and

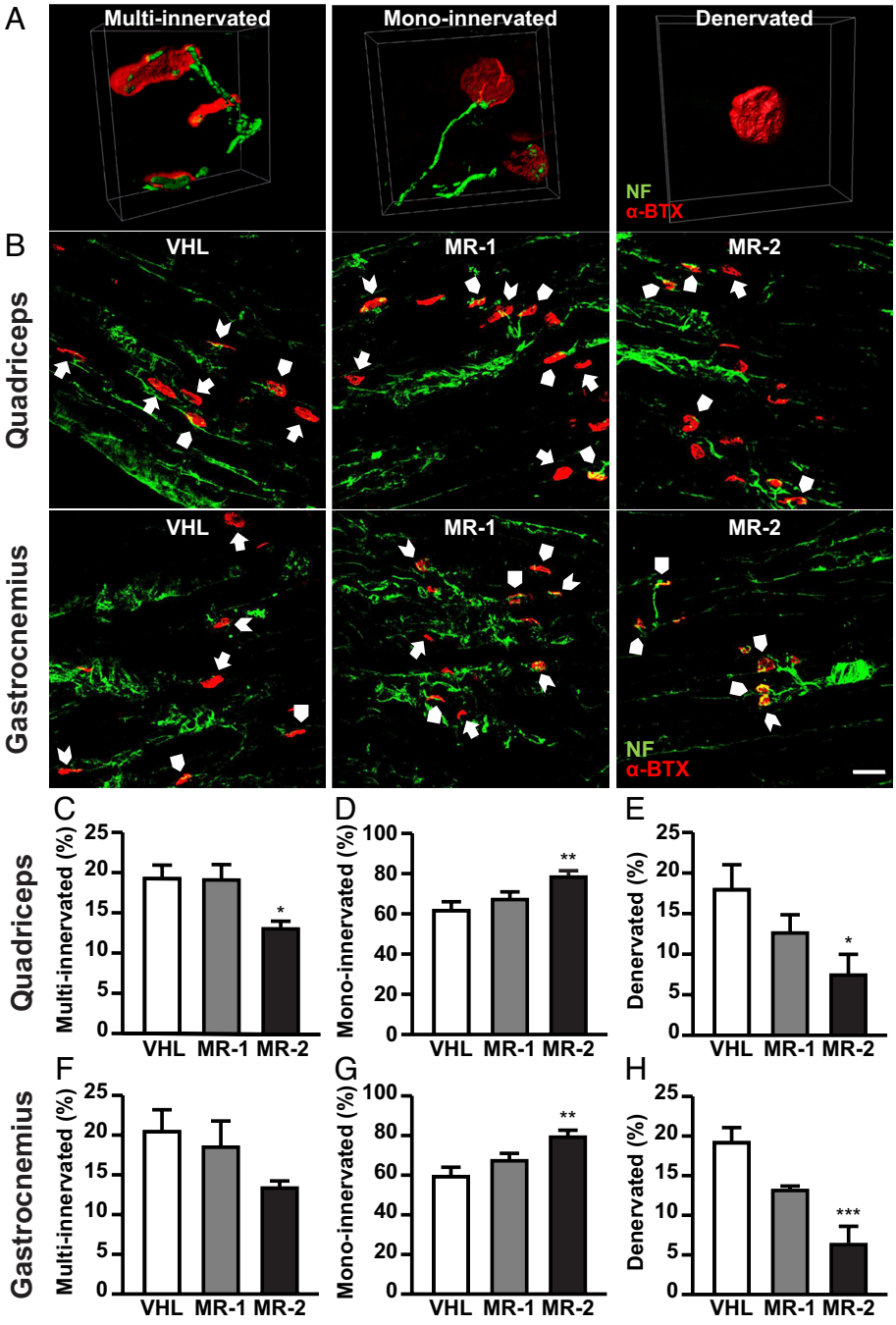

Fig. 4. Effect of MR-409 on NMJ maturation/innervation in P12 SMA mice. (*A*) Representative confocal microscopy images of multi-innervated, mono-innervated, and denervated NMJs reconstructed using the isosurface module of Imaris software (Bitplane). Postsynaptic acetylcholine receptors were labeled with α-BTX (red) while the presynaptic terminal was labeled with anti-NF (green). (*B*) Representative longitudinal sections of quadriceps and gastrocnemius stained with anti-NF (green) and α-BTX (red). Multi-innervated (arrowheads), mono-innervated (arrow pentagons), and denervated (arrows) NMJs are indicated. (Scale bar, 25 μm.) Quantification of multi-innervated (*C* and *F*), mono-innervated (*D* and *G*), and denervated (*E* and *H*) endplates in quadriceps and gastrocnemius. Data are mean ± SEM. $*P < 0.05$, $**P < 0.01$, $***P < 0.001$ vs. VHL by one-way ANOVA and Tukey's post hoc test ($n = 5$ for each group).

gastrocnemius, along with enhanced NMJ maturation and reduced degeneration of MNs in the spinal cord. Indeed, treatment with MR-409 attenuated muscle atrophy and promoted an increase in fiber size, as revealed by analysis of mean fiber area, perimeter, and maximum Feret's diameter (46). Notably, the highest dose of MR-409 induced an almost complete rescue of SMA muscle phenotype, as evidenced by the comparison with WT animals.

Although αMN loss-related denervation is a prominent feature in SMA, growing evidence suggests that muscle atrophy is also caused by muscle-autonomous alterations, which contribute to the motor defects characteristic of the disease. In fact, muscle-specific ablation of SMN protein, without reduction in αMN can result in massive muscular dystrophy (47). Similarly, muscle-specific *Smn* depletion in mice induces morphological alterations in myofibers and NMJs, with compromised motor function and reduced lifespan (32). Furthermore, abnormal expression of markers for skeletal muscle development and maintenance, such as myosins, and dysregulation of the myogenic program have been demonstrated in SMA (11, 34, 37, 48). Indeed, MyoD and myogenin levels have been found increased in SMA, likely as an adaptive mechanism to prevent muscle atrophy (49, 50). In addition, it has

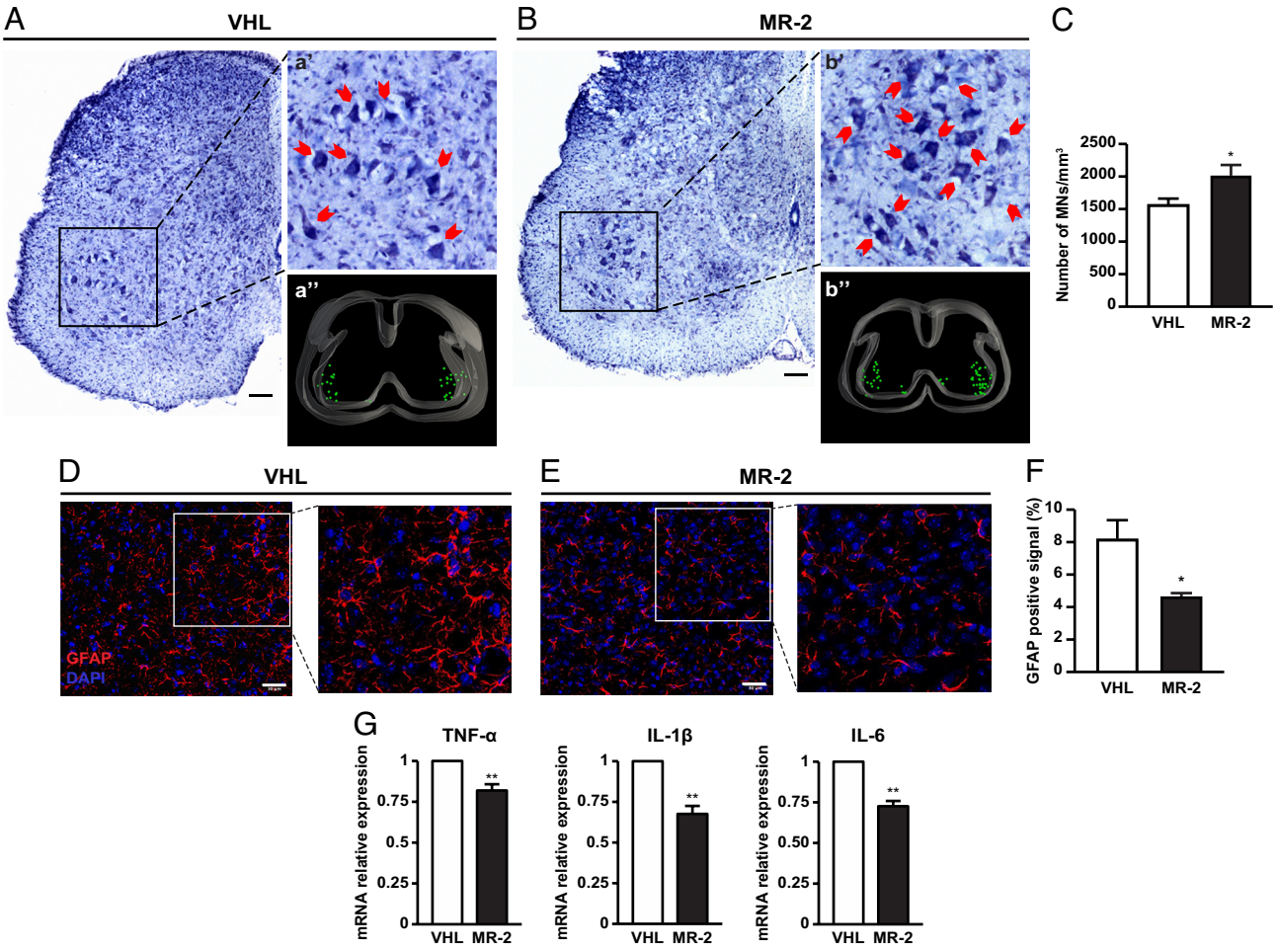

Fig. 5. Effect of MR-409 on motor neuron survival and astrogliosis in P12 SMA mice. Representative Nissl-stained sections of lumbar spinal cord from VHL (*A*) and 2 mg/kg MR-409 (MR-2) (*B*) mice. (*a'* and *b'*) αMNs indicated by red arrows in the magnified views. (*a''* and *b''*) Representative spinal cord 3D reconstructions obtained by Stereo Investigator software: αMNs are represented as green spots in the ventral horns. (Scale bar, 50 μm.) (*C*) Quantification of MN number/mm^3. Data are mean ± SEM. *$P < 0.05$ vs. VHL by unpaired Student's *t* test ($n = 5$ for each group). Representative confocal micrographs of GFAP immunostaining (red) in ventral horns of lumbar spinal cord of mice of mice treated with VHL (*D*) or MR-209 (*E*). Nuclei are stained in blue with DAPI. (Scale bar, 30 μm.) (*F*) Bar graph showing the percentage of GFAP positive astrocytes. Data are mean ± SEM. *$P < 0.05$ vs. VHL by unpaired Student's *t* test ($n = 3$ for each group). (*G*) Real-time PCR analysis for *TNF-αIL-1β* and *IL-6* in spinal cord of VHL MR-2 mice. Results, normalized to *18S rRNA*, are mean ± SEM. **$P < 0.01$ vs. VHL by unpaired Student's *t* test ($n = 3$ for each group).

been shown that in denervated muscle cells and in muscle of mice and humans with SMA, myogenin controls muscle atrophy by enhancing the expression of MuRF1 and atrogin-1, thereby promoting proteolysis (38, 51). We demonstrate that MR-409 increased Myod1 and myogenin transcripts in quadriceps and gastrocnemius of SMA mice, compared with VHL-treated animals. However, there was a concomitant reduction in atrogin-1 and MuRF1 mRNA and protein, suggesting that myogenin elevation is not associated with muscular degradation. Accordingly, MR-409 upregulated the expression of genes essential for muscle function, such as slow and fast myosins, whose levels are generally altered in SMA (11, 34, 37, 48). Overall, these results indicate that MR-409 counteracts muscle atrophy. This is in agreement with our previous findings showing the ability of GHRH(1–44)NH_2 to prevent cytokine-induced atrophy in skeletal myotubes through inhibition of apoptotic and proteolytic pathways and via receptor-mediated mechanisms (21). Moreover, we and others have previously demonstrated the cardioprotective activities of both GHRH (1–44)NH_2 and its agonistic analogs (17, 19, 23, 52), possibly suggesting an additional role of MR-409 in counteracting SMA-related heart defects (7). The presence of GHRH-R in both muscle and spinal cord of SMA mice further sustains our findings, since MR-409 possesses high binding affinity for this receptor (22). Interestingly, activation of GHRH-R promotes cAMP elevation, which has been implicated in the protective effect of GHRH and its agonistic analogs in different in vitro and in vivo models of disease, including ischemic stroke and neurodegeneration (17, 19, 23, 26, 28). Moreover, GHRH belongs to the family of the so-called brain-gut peptides, which also includes pituitary adenylate cyclase-activating polypeptide, a neuropeptide with beneficial effects in models of spinal cord injury, spinal and bulbar muscular atrophy and Huntington disease, acting via cAMP-mediated mechanisms (15, 53). Although we did not address it in this study, we assume that the cAMP pathway may be involved in the protective effects of MR-409, along with others activated by GHRH-R, such as PI3K/Akt, GSK-3b, mTOR, and MAPK/ERK (19, 21, 28), which are also protective in SMA (54).

The NMJ is a highly specialized synapse between a MN nerve terminal and its muscle fiber, transmitting the impulses produced by the MN and allowing the muscle fiber contraction. NMJ breakdown is generally recognized as an early event in SMA pathogenesis, likely even anticipating αMN degeneration and motor dysfunction. In fact, in both SMA patients and animal models, NMJs show defects such as NF accumulation at presynaptic terminals, smaller

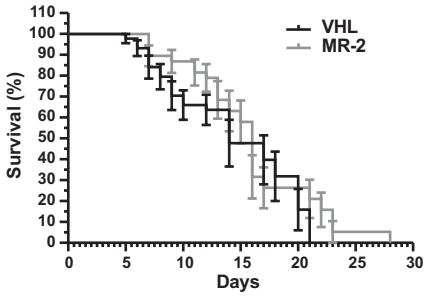

Fig. 6. Effect of MR-409 on survival of SMA mice. Kaplan–Meier survival curves of SMA mice treated with either VHL or MR-2 (VHL: *n* = 44; MR-2: *n* = 38).

and immature endplates and reduced transmitter release. The persistence of polyneuronal innervation is a characteristic of incorrect/delayed NMJ development in SMA; moreover, neuromuscular denervation in vulnerable muscles results in severe muscle atrophy, likely due to defects in synapse maintenance (2, 5, 39, 55). Thus, one potential therapeutic strategy to counteract the progression of SMA is to improve NMJ defects by promoting postsynaptic differentiation and preventing αMN degeneration. Our results, showing an increase in the percentage of mono-innervated endplates, and a concomitant decrease in those multi-innervated and denervated in SMA mice, suggest that MR-409 promotes NMJ maturation, which, in turn, may positively affect muscle trophism.

Degeneration and death of αMNs within the anterior horns of the spinal cord and brainstem are key pathological features of SMA, already evident at pre-symptomatic stages, hence preceding the disease onset in SMNΔ7 mice (2, 4, 40, 41). Such neurodegeneration further contributes to muscle weakness and atrophy (2, 6). While some studies showed that both peripheral and central synaptic defects are autonomously caused by insufficient levels of SMN in αMNs (8, 56), others indicated that increasing SMN levels in αMNs, although sufficient to restore both NMJ and synaptic integrity, only partially improved the SMA phenotype, suggesting a role for peripheral tissues in SMA pathogenesis (10, 35). Accordingly, although a positive trend was observed, SMN protein levels were not significantly increased in spinal cords of SMA mice treated with MR-409. Moreover, our results demonstrate that, in addition to promoting NMJ maturation, MR-409 efficiently counteracts αMN loss in spinal cord of SMA mice, compared with untreated mice. Interestingly, both autophagy and apoptosis have been implicated in αMN death in SMA (57, 58). In addition, although the role of autophagy remains to be explored, MR-409 has been recently found to inhibit apoptosis of neural stem cells exposed to oxygen-glucose deprivation/reoxygenation (28), a protective mechanism that could take place also in αMNs. On the one side, our findings highlight the importance of the cross talk between the muscle fibers and αMNs and on the other side, they indicate a neuroprotective role of MR-409, as already demonstrated in other experimental models (17, 27–29). Of note, neurotrophic factors released by skeletal muscle cells (presumably in response to MR-409) could also sustain the survival of αMNs (59).

It is well known that astrocytes and microglia activate in response to inflammatory stimuli and promote neuroinflammation, resulting in cytokine production, immune infiltration and activation of proapoptotic pathways (9). Other studies support the contribution of astrocytes to SMA pathogenesis. Indeed, an increase in GFAP immunoreactivity as a marker for astrocyte activation has been observed in SMA patients and SMNΔ7 mice, along with increased mRNA levels of inflammatory cytokines (42, 60). Moreover, activation of astrocytes in the spinal cord of SMA mouse and human SMA induced pluripotent stem cells (iPSCs) was detected before overt αMN loss, suggesting that astrogliosis may contribute to αMN dysfunction (61). Here, we show that MR-409 attenuated neuroinflammation in the spinal cord of SMA mice, as demonstrated by both reduced GFAP immunoreactivity and downregulation of inflammatory cytokine transcript levels. This finding is in line with a recent study by Liu et al., where s.c. treatment with MR-409, improved neurological functional recovery and attenuated neuroinflammation in a mouse model of ischemic stroke (28). In fact, in the above study MR-409 was administered at doses equivalent to 0.5 and 1 mg/kg. Accordingly, in SMA mice, MR-409 was initially used at 0.5 mg/kg, showing little or no effect; thus, we subsequently tested 1 mg/kg and 2 mg/kg doses. Although some positive outcomes were observed with 1 mg/kg MR-409, the highest dose was the most effective, which is not surprising, considering the severity of this model of SMA.

Overall, the beneficial effects of MR-409 in SMA mice were accompanied by a slight, but not significant, increase in life expectancy, compared with VHL-treated mice. Based on these results, we hypothesize that MR-409, rather than targeting the expression of SMN protein, whose levels in the spinal cord were unchanged, acts on peripheral districts such as the skeletal muscle, along with displaying neuroprotective and anti-inflammatory activities in the CNS.

In conclusion, the present study provides evidence demonstrating that MR-409 may be a promising agent for the treatment of SMA. In fact, despite encouraging results coming from gene therapy and ASO approaches, additional treatments are needed, such as combined therapies with drugs targeting SMN-independent factors, including molecules that act to increase muscle trophism and neuroprotection.

Materials and Methods

Please see *SI Appendix, Materials and Methods* for more information.

Animal Model. *SMNΔ7*$^{+/+}$; *SMN2*$^{+/+}$; *Smn*$^{+/-}$ mice (stock number 005025; Jackson Laboratory) were interbred to obtain *Smn*$^{-/-}$ offspring (SMA mice, as model of type II SMA). Pups were tail snipped at postnatal day 0 (P0) for the identification and genotyped by PCR assay according to the protocol provided by Jackson Laboratory. SMA pups were maintained in the cage with the mother until the sacrifice at P12, under standard conditions with 12/12-h light/dark cycle and free access to food and water. Another group of SMA mice was used for survival analysis. All efforts have been made to minimize the number of animals and their suffering levels. Pups of both sexes were used in this study. All experimental procedures were performed in strict accordance with institutional guidelines in compliance with national (D.L. N.26, 04/03/2014) and international law and policies (new directive 2010/63/EU). The study was approved by the Italian Ministry of Health (protocol #980/2020-PR). Additionally, the ad hoc Ethical Committee of the University of Turin approved this study. A total of 102 SMA mice were used and 3 WT mice; moreover, 11 SMA animals died prematurely before P12 and could not be used for the ex vivo analysis. All the analyses were performed blinded for the treatment of the mice.

Peptide Administration. GHRH-R agonist MR-409 [N-Me-Tyr^{1}, D-Ala^{2}, Orn^{12}, Abu^{15}, Orn^{21}, Nle^{27}, Asp^{28})-hGHRH(1–29)NH-CH$_3$)] was synthesized and purified in the laboratory of one of us (A.V.S.), as described previously (22). P2 SMA mice were randomly divided into three groups, independently from the gender: VHL (*n* = 44), MR-1 (*n* = 20) and MR-2 (*n* = 38). MR-409, dissolved in 0.1% DMSO and 10% aqueous propylene glycol solution (VHL solution), was administered s.c. daily at the dose of 1 mg/kg (MR-1 group) or 2 mg/kg (MR-2 group) from P2 until euthanization. Mice of the VHL group were treated using VHL solution without drugs. Animals were euthanized at P12 and used for survival study.

Behavioral Assessment. Behavioral tests were performed to evaluate phenotypic features and motor performance of mice treated with MR-409 compared with VHL, as described previously (62). Animals underwent tail suspension, righting reflex, hindlimb suspension, and negative geotaxis tests.

Real-time PCR. Total RNA extraction and reverse transcription to cDNA (1 μg RNA) from frozen tissues were performed as previously described (23). For real-time PCR, cDNAs were treated with DNA-free DNase (Life Technologies) and reaction performed with 50 ng cDNA, 100 nM of each primer and the Luna Universal qPCR Master Mix (New England BioLabs) using ABI-Prism 7300 (Applied Biosystems). Real-time PCR analysis was performed as described previously (21, 23).

Western Blot Analysis. Proteins, obtained from tissue lysates, were resolved in 11% Sodium Dodecyl Sulphate - PolyAcrylamide Gel Electrophoresis (SDS-PAGE), as previously described (19, 21, 23). Membranes were incubated with rabbit polyclonal primary antibody for MuRF1 (1:500; ref: Ab77577, Abcam), GHRH-R (1:500; ref: Ab28692, Abcam) or SMN (1:2,000, ref: 610646, BD Biosciences). Blots were reprobed with mouse monoclonal anti-actin antibody (1:500; ref: sc–376421, Santa Cruz Biotechnology) for normalization. Immunoreactive proteins were visualized using horseradish peroxidase-conjugated goat anti-mouse or goat anti-rabbit (1:4,000) antibodies (Southern Biotech) by enhanced chemiluminescence using ChemiDoc XRS (Bio-Rad). Densitometric analysis was performed with Quantity One software (Bio-Rad).

Histochemistry. Sections (40 μm thick) of quadriceps and gastrocnemius were analyzed after hematoxylin/eosin (H/E) staining using Neurolucida software (MBF Bioscience). Lumbar spinal cord slices (40 μm-thick) were Nissl-stained with Cresyl Violet acetate (Sigma-Aldrich), as previously described (46, 58). For αMN counting, spinal cord slices (L4-L5, 1 section every 320 μm) were analyzed using a stereological technique, the Optical Fractionator, a computer-assisted microscope and the Stereo Investigator software (MBF Bioscience).

Immunofluorescence Analysis. Tissues sections were incubated overnight at 4 °C with specific primary antibodies (see below), then with fluorochrome-conjugated secondary antibodies (Cy™3 AffiniPure anti-rabbit (1:300), ref: 711165152; Alexafluor anti-mouse 488 (1:200), ref: 715545150; Jackson ImmunoResearch Laboratories). For the NMJ analysis, muscle slices were incubated for 30 min at room temperature with α-BTX Alexa Fluor 555, followed by anti-NF antibody (anti NF-M; mouse, 1:500; ref: MAB1621, Millipore), overnight. Representative images were acquired with a Leica TCS-SP5 confocal laser scanning microscope (Leica Microsystems). The activation of astrocyte in ventral horns sections was analyzed by confocal laser scanning microscope. The percentage of the overall GFAP-positive cells (anti-GFAP; rabbit, 1:500; ref: Z0334, DAKO Cytomation) was quantified using ImageJ software.

Statistical Analysis. Results are expressed as mean ± SEM. Statistical significance was determined by using 1-way ANOVA with Tukey's or Dunnett's post hoc analysis for multiple groups or unpaired two-tailed Student's *t* test to compare two groups when appropriate. Repeated measures ANOVA, mixed-effects model with the Geisser-Greenhouse correction, followed by Tukey's multiple comparisons post hoc test, and contingency table analysis (Fisher's exact test) were used for behavioral tests. Animal lifespan was calculated by Kaplan–Meier survival curve (censoring the mice that were sacrificed at P12). Analysis were performed using GraphPad Prism 8.0 (GraphPad Software). Significance was established for $P < 0.05$.

Data, Materials, and Software Availability. All study data are included in the article and/or *SI Appendix*.

ACKNOWLEDGMENTS. This work was supported by the Italian Ministry of Education, University and Research (Ministero dell'Istruzione, dell'Università e della Ricerca, MIUR) (N. 2017HRTZYA) to R.G. and (N. 2017S55RXB) to E.G.; University of Turin (Ex-60% 2020) to I.G. MIUR project "Dipartimenti di Eccellenza 2018-2022" to the Department of Medical Sciences (project N. D15D18000410001) and to the Department of Neurosciences "Rita Levi Montalcini" (University of Turin) and Girotondo/ONLUS and SMArathon-ONLUS foundation grants to A.V.S. and M.B. The work in the laboratory of A.V.S. was supported by the Medical Research Service of the Veterans Affairs Department and University of Miami Miller School of Medicine.

Author affiliations: [a]Department of Neuroscience "Rita Levi Montalcini", Neuroscience Institute Cavalieri Ottolenghi, University of Turin, 10043 Turin, Italy; [b]Division of Endocrinology, Diabetes and Metabolism, Department of Medical Sciences, University of Turin, 10126 Turin, Italy; [c]Department of Pharmacy, G. d'Annunzio University, 66100 Chieti, Italy; [d]Endocrine, Polypeptide, and Cancer Institute, Veterans Affairs Medical Center, Miami, FL 33125; [e]South Florida VA Foundation for Research and Education, Veterans Affairs Medical Center, Miami, FL 33125; [f]Divisions of Medical/Oncology and Endocrinology, Department of Medicine, Miller School of Medicine, University of Miami, Miami, FL 33136; [g]Department of Pathology, Miller School of Medicine, University of Miami, Miami, FL 33136; and [h]Sylvester Comprehensive Cancer Center, Miller School of Medicine, University of Miami, Miami, FL 33136

Author contributions: M.B., I.G., and R.G. designed research; M.B., I.G., A.C., F.P., R.S., and S.L. performed research; M.B., R.C., W.S., A.V.S., and A.V. contributed new reagents/analytic tools; M.B., I.G., A.C., F.P., R.S., S.L., E.G., A.V.S., A.V., and R.G. analyzed data; and M.B., E.G., A.V.S., and R.G. wrote the paper.

1. I. E. C. Verhaart *et al.*, Prevalence, incidence and carrier frequency of 5q-linked spinal muscular atrophy - A literature review. *Orphanet. J. Rare. Dis.* **12**, 124 (2017).
2. E. Mercuri, M. C. Pera, M. Scoto, R. Finkel, F. Muntoni, Spinal muscular atrophy-insights and challenges in the treatment era. *Nat. Rev. Neurol.* **16**, 706–715 (2020).
3. S. Lefebvre *et al.*, Identification and characterization of a spinal muscular atrophy-determining gene. *Cell* **80**, 155–165 (1995).
4. C. L. Lorson, H. Rindt, M. Shababi, Spinal muscular atrophy: Mechanisms and therapeutic strategies. *Hum. Mol. Genet.* **19**, R111–R118 (2010).
5. M. Boido, A. Vercelli, Neuromuscular junctions as key contributors and therapeutic targets in spinal muscular atrophy. *Front. Neuroanat.* **10**, 6 (2016).
6. K. Talbot, E. F. Tizzano, The clinical landscape for SMA in a new therapeutic era. *Gene. Ther.* **24**, 529–533 (2017).
7. M. Shababi, C. L. Lorson, S. S. Rudnik-Schoneborn, Spinal muscular atrophy: A motor neuron disorder or a multi-organ disease? *J. Anat.* **224**, 15–28 (2014).
8. R. G. Gogliotti *et al.*, Motor neuron rescue in spinal muscular atrophy mice demonstrates that sensory-motor defects are a consequence, not a cause, of motor neuron dysfunction. *J. Neurosci.* **32**, 3818–3829 (2012).
9. E. Abati, G. Citterio, N. Bresolin, G. P. Comi, S. Corti, Glial cells involvement in spinal muscular atrophy: Could SMA be a neuroinflammatory disease? *Neurobiol. Dis.* **140**, 104870 (2020).
10. Y. Hua *et al.*, Motor neuron cell-nonautonomous rescue of spinal muscular atrophy phenotypes in mild and severe transgenic mouse models. *Genes. Dev.* **29**, 288–297 (2015).
11. S. Jablonka, L. Hennlein, M. Sendtner, Therapy development for spinal muscular atrophy: Perspectives for muscular dystrophies and neurodegenerative disorders. *Neurol. Res. Pract.* **4**, 2 (2022).
12. S. Messina *et al.*, Spinal muscular atrophy: State of the art and new therapeutic strategies. *Neurol. Sci.*, 10.1007/s10072-021-05258-3 (2021).
13. G. Menduti, D. M. Rasa, S. Stanga, M. Boido, Drug screening and drug repositioning as promising therapeutic approaches for spinal muscular atrophy treatment. *Front. Pharmacol.* **11**, 592234 (2020).
14. M. Van Alstyne *et al.*, Gain of toxic function by long-term AAV9-mediated SMN overexpression in the sensorimotor circuit. *Nat. Neurosci.* **24**, 930–940 (2021).
15. E. Zuccaro, D. Piol, M. Basso, M. Pennuto, Motor neuron diseases and neuroprotective peptides: A closer look to neurons. *Front. Aging. Neurosci.* **13**, 723871 (2021).
16. R. Guillemin *et al.*, Growth hormone-releasing factor from a human pancreatic tumor that caused acromegaly. *Science* **218**, 585–587 (1982).
17. A. V. Schally *et al.*, Actions and potential therapeutic applications of growth hormone-releasing hormone agonists. *Endocrinology* **160**, 1600–1612 (2019).
18. R. Granata, Peripheral activities of growth hormone-releasing hormone. *J. Endocrinol. Invest.* **39**, 721–727 (2016).
19. R. Granata *et al.*, Growth hormone-releasing hormone promotes survival of cardiac myocytes in vitro and protects against ischaemia-reperfusion injury in rat heart. *Cardiovasc. Res.* **83**, 303–312 (2009).
20. C. Penna *et al.*, GH-releasing hormone induces cardioprotection in isolated male rat heart via activation of RISK and SAFE pathways. *Endocrinology* **154**, 1624–1635 (2013).
21. D. Gallo *et al.*, GH-releasing hormone promotes survival and prevents TNF-alpha-induced apoptosis and atrophy in C2C12 myotubes. *Endocrinology* **156**, 3239–3252 (2015).
22. R. Cai *et al.*, Synthesis of new potent agonistic analogs of growth hormone-releasing hormone (GHRH) and evaluation of their endocrine and cardiac activities. *Peptides* **52**, 104–112 (2014).
23. I. Gesmundo *et al.*, Growth hormone-releasing hormone attenuates cardiac hypertrophy and improves heart function in pressure overload-induced heart failure. *Proc. Natl. Acad. Sci. U.S.A.* **114**, 12033–12038 (2017).
24. P. Xiang *et al.*, Improvement of cardiac and systemic function in old mice by agonist of growth hormone-releasing hormone. *J. Cell Physiol.* **236**, 8197–8207 (2021).
25. A. C. Rieger *et al.*, Growth hormone-releasing hormone agonists ameliorate chronic kidney disease-induced heart failure with preserved ejection fraction. *Proc. Natl. Acad. Sci. U.S.A.* **118**, e2019835118 (2021).
26. X. Zhang *et al.*, Beneficial effects of growth hormone-releasing hormone agonists on rat INS-1 cells and on streptozotocin-induced NOD/SCID mice. *Proc. Natl. Acad. Sci. U.S.A.* **112**, 13651–13656 (2015).
27. M. C. Thounaojam *et al.*, Protective effects of agonists of growth hormone-releasing hormone (GHRH) in early experimental diabetic retinopathy. *Proc. Natl. Acad. Sci. U.S.A.* **114**, 13248–13253 (2017).
28. Y. Liu *et al.*, Agonistic analog of growth hormone-releasing hormone promotes neurofunctional recovery and neural regeneration in ischemic stroke. *Proc. Natl. Acad. Sci. U.S.A.* **118**, e2109600118 (2021).
29. L. Recinella *et al.*, Antinflammatory, antioxidant, and behavioral effects induced by administration of growth hormone-releasing hormone analogs in mice. *Sci. Rep.* **10**, 732 (2020).
30. M. E. Butchbach, J. D. Edwards, A. H. Burghes, Abnormal motor phenotype in the SMNDelta7 mouse model of spinal muscular atrophy. *Neurobiol Dis.* **27**, 207–219 (2007).
31. T. T. Le *et al.*, SMNDelta7, the major product of the centromeric survival motor neuron (SMN2) gene, extends survival in mice with spinal muscular atrophy and associates with full-length SMN. *Hum. Mol. Genet.* **14**, 845–857 (2005).
32. J. K. Kim *et al.*, Muscle-specific SMN reduction reveals motor neuron-independent disease in spinal muscular atrophy models. *J. Clin. Invest.* **130**, 1271–1287 (2020).

33. V. Valsecchi, M. Boido, E. De Amicis, A. Piras, A. Vercelli, Expression of muscle-specific MiRNA 206 in the progression of disease in a murine SMA model. *PLoS One* **10**, e0128560 (2015).
34. J. G. Boyer *et al.*, Myogenic program dysregulation is contributory to disease pathogenesis in spinal muscular atrophy. *Hum. Mol. Genet.* **23**, 4249–4259 (2014).
35. Y. I. Lee, M. Mikesh, I. Smith, M. Rimer, W. Thompson, Muscles in a mouse model of spinal muscular atrophy show profound defects in neuromuscular development even in the absence of failure in neuromuscular transmission or loss of motor neurons. *Dev. Biol.* **356**, 432–444 (2011).
36. P. S. Zammit, Function of the myogenic regulatory factors Myf5, MyoD, Myogenin and MRF4 in skeletal muscle, satellite cells and regenerative myogenesis. *Semin. Cell Dev. Biol.* **72**, 19–32 (2017).
37. R. Martinez-Hernandez, S. Bernal, L. Alias, E. F. Tizzano, Abnormalities in early markers of muscle involvement support a delay in myogenesis in spinal muscular atrophy. *J. Neuropathol. Exp. Neurol.* **73**, 559–567 (2014).
38. K. V. Bricceno *et al.*, Histone deacetylase inhibition suppresses myogenin-dependent atrogene activation in spinal muscular atrophy mice. *Hum. Mol. Genet.* **21**, 4448–4459 (2012).
39. S. Kariya *et al.*, Reduced SMN protein impairs maturation of the neuromuscular junctions in mouse models of spinal muscular atrophy. *Hum. Mol. Genet.* **17**, 2552–2569 (2008).
40. H. K. Shorrock, T. H. Gillingwater, E. J. N. Groen, Molecular mechanisms underlying sensory-motor circuit dysfunction in SMA. *Front. Mol. Neurosci.* **12**, 59 (2019).
41. P. d'Errico *et al.*, Selective vulnerability of spinal and cortical motor neuron subpopulations in delta7 SMA mice. *PLoS One* **8**, e82654 (2013).
42. H. Rindt *et al.*, Astrocytes influence the severity of spinal muscular atrophy. *Hum. Mol. Genet.* **24**, 4094–4102 (2015).
43. L. Recinella *et al.*, Growth hormone-releasing hormone antagonistic analog MIA-690 stimulates food intake in mice. *Peptides* **142**, 170582 (2021).
44. F. J. Vaccarino, F. E. Bloom, J. Rivier, W. Vale, G. F. Koob, Stimulation of food intake in rats by centrally administered hypothalamic growth hormone-releasing factor. *Nature* **314**, 167–168 (1985).
45. T. Imaki *et al.*, The satiety effect of growth hormone-releasing factor in rats. *Brain Res.* **340**, 186–188 (1985).
46. M. Boido *et al.*, Increasing agrin function antagonizes muscle atrophy and motor impairment in spinal muscular atrophy. *Front. Cell Neurosci.* **12**, 17 (2018).
47. C. Cifuentes-Diaz *et al.*, Deletion of murine SMN exon 7 directed to skeletal muscle leads to severe muscular dystrophy. *J. Cell Biol.* **152**, 1107–1114 (2001).
48. K. V. Bricceno *et al.*, Survival motor neuron protein deficiency impairs myotube formation by altering myogenic gene expression and focal adhesion dynamics. *Hum. Mol. Genet.* **23**, 4745–4757 (2014).
49. M. Ishido, K. Kami, M. Masuhara, In vivo expression patterns of MyoD, p21, and Rb proteins in myonuclei and satellite cells of denervated rat skeletal muscle. *Am. J. Physiol. Cell Physiol.* **287**, C484–C493 (2004).
50. J. P. Hyatt, R. R. Roy, K. M. Baldwin, V. R. Edgerton, Nerve activity-independent regulation of skeletal muscle atrophy: Role of MyoD and myogenin in satellite cells and myonuclei. *Am. J. Physiol. Cell Physiol.* **285**, C1161–C1173 (2003).
51. V. Moresi *et al.*, Myogenin and class II HDACs control neurogenic muscle atrophy by inducing E3 ubiquitin ligases. *Cell* **143**, 35–45 (2010).
52. R. M. Kanashiro-Takeuchi *et al.*, Cardioprotective effects of growth hormone-releasing hormone agonist after myocardial infarction. *Proc. Natl. Acad. Sci. U.S.A.* **107**, 2604–2609 (2010).
53. I. Soles-Tarres *et al.*, Pituitary adenylate cyclase-activating polypeptide (PACAP) protects striatal cells and improves motor function in Huntington's disease models: Role of PAC1 receptor. *Front. Pharmacol.* **12**, 797541 (2021).
54. O. Biondi *et al.*, In vivo NMDA receptor activation accelerates motor unit maturation, protects spinal motor neurons, and enhances SMN2 gene expression in severe spinal muscular atrophy mice. *J. Neurosci.* **30**, 11288–11299 (2010).
55. K. K. Ling, R. M. Gibbs, Z. Feng, C. P. Ko, Severe neuromuscular denervation of clinically relevant muscles in a mouse model of spinal muscular atrophy. *Hum. Mol. Genet.* **21**, 185–195 (2012).
56. T. L. Martinez *et al.*, Survival motor neuron protein in motor neurons determines synaptic integrity in spinal muscular atrophy. *J. Neurosci.* **32**, 8703–8715 (2012).
57. A. Piras *et al.*, Inhibition of autophagy delays motoneuron degeneration and extends lifespan in a mouse model of spinal muscular atrophy. *Cell Death Dis.* **8**, 3223 (2017).
58. R. Schellino, M. Boido, T. Borsello, A. Vercelli, Pharmacological c-Jun NH2-terminal kinase (JNK) pathway inhibition reduces severity of spinal muscular atrophy disease in mice. *Front. Mol. Neurosci.* **11**, 308 (2018).
59. D. Bottai, R. Adami, Spinal muscular atrophy: New findings for an old pathology. *Brain. Pathol.* **23**, 613–622 (2013).
60. C. Cervero *et al.*, Glial activation and central synapse loss, but not motoneuron degeneration, are prevented by the Sigma-1 receptor agonist PRE-084 in the Smn2B/- mouse model of spinal muscular atrophy. *J. Neuropathol. Exp. Neurol.* **77**, 577–597 (2018).
61. J. V. McGivern *et al.*, Spinal muscular atrophy astrocytes exhibit abnormal calcium regulation and reduced growth factor production. *Glia* **61**, 1418–1428 (2013).
62. B. F. El-Khodor *et al.*, Identification of a battery of tests for drug candidate evaluation in the SMNDelta7 neonate model of spinal muscular atrophy. *Exp. Neurol.* **212**, 29–43 (2008).